Electrospun Fiber Membranes of Novel Thermoplastic Polyester Elastomers: Preparation and Characterization

Ding Cao,[1] Zhifeng Fu,[1] Congju Li[2]

[1]*State Key Laboratory of Chemical Resource Engineering, Beijing University of Chemical Technology, Beijing 100029, People's Republic of China*
[2]*Beijing Key Laboratory of Clothing Materials R&D and Assessment, College of Material Science and Engineering, Beijing Institute of Fashion Technology, Beijing 100029, People's Republic of China*

Received 1 November 2009; accepted 26 December 2010
DOI 10.1002/app.34024
Published online 1 June 2011 in Wiley Online Library (wileyonlinelibrary.com).

ABSTRACT: Electrospinning nanotechnology has recently attracted lots of attention in different kinds of applications. Poly(butylene terephthalate) random-segment copolymers, named poly[(butylene terephthalate)-*co*-(1,4-cyclohexanedimethanol terephthalate)]-*b*-poly(tetramethylene glycol) (P(BT-*co*-CT)-*b*-PTMG), were synthesized in this study. On the basis of the new thermoplastic polyester elastomers (TPEEs), the fiber membranes were subsequently electrospun. With the aid of a cosolvent of trifluoroacetic acid and dichloromethane, the resulting solutions with a concentration between 24 and 32% w/v were electrospun into fibers without beads. The results also show a good spinnability for the copolymer solution in a range of voltages from 16 to 24 kV. When the molar ratio of 1,4-cyclohexanedimethanol to 1,4-butanediol was 10 : 90, the electrospun membrane prepared by the corresponding copolymers had a higher elastic modulus than the commercial TPEE (Hytrel 4056, 4.51 ± 0.35 MPa). Differential scanning calorimetry and X-ray diffraction showed that a crystalline phase existed in the electrospun poly[(butylene terephthalate)-*co*-(1,4-cyclohexanedimethanol terephthalate)]-*b*-poly(tetramethylene glycol) (P(BT-*co*-CT)-*b*-PTMG) copolymer fiber membranes. The melting point of the electrospun fibers was approximately less than that of the corresponding copolymers © 2011 Wiley Periodicals, Inc. J Appl Polym Sci 122: 1698–1706, 2011

Key words: membranes; nanotechnology; polycondensation

INTRODUCTION

Recently, the electrospinning method has attracted a great deal of attention for the preparation of ultrafine polymer fibers and nonwoven membranes. This technique was first studied by Zeleny in 1914 and patented by Formhals[1] in 1934. The parameters that highly determine the morphology and the physical properties of fibers (or membranes) have been gradually investigated.[2,3] The effect of the solution properties on electrospinning were reported by Fong et al.[4] and Lee et al.[5] Also, the applied electric field[6] and ambient conditions[7] have been found to affect the morphology of the electrospun fibers. The formation mechanism of fibers during electrospinning is another hotspot in fiber research.[3,8] The surface tension, net charge density, and rapidly whipping fluid jet of the polymer solution play important parts in the processing of the fibers.[3,9,10]

Up to now, a lot of polymers have been successfully electrospun into fibers, and electrospun polymer fibers with diameters as small as 5 nm have been prepared.[11] Considering the unusually high porosity in their nanometer-scale architecture and large surface area, electrospun materials have been proved to be useful in the medical field for vascular grafts, prosthetic blood vessels, and tissue engineering scaffolds and in the water-treatment industry for filtration applications.[6,8,12]

Poly(butylene terephthalate) (PBT) is a commercial polyester with excellent mechanical properties, especially tensile strength. The incorporation of poly(ethylene glycol) (PEG) or poly(tetramethylene glycol) (PTMG) into PBT as soft segments can adjust the mechanical and thermal properties of polymeric materials. With PTMG as the soft segment, better mechanical properties are expected because it is well known that the thermal and

Correspondence to: Z. Fu (fuzf@mail.buct.edu.cn) or C. Li (congjuli@gmail.com).

Contract grant sponsor: Natural Science Foundation of China; contract grant number: 51073005.
Contract grant sponsor: Beijing Natural Science Foundation; contract grant numbers: 2112013, KZ201010012012
Funding Project for Academic Human Resources Development in Institutions of Higher Learning Under the Jurisdiction of Beijing Municipality [PHR(IHLB)].
Contract grant sponsor: PHR (IHLB).
Contract grant sponsor: 863 Project; contract grant number: 2007AA021906.
Contract grant sponsor: 973 Project; contract grant number: 2010CB933501.

mechanical properties of PTMG are better than those of the other polyglycols, such as PEG and poly (propylene glycol), when it is transformed to a segmented block copolymer.[13,14] However, the soft-segment length (e.g., PEG) is limited at 1000 Da, and its mass content is between 60 and 80 wt %.[15] It is not reasonable to decrease the length of the soft segments solely by a decrease in its content in the copolymer chains. Fortunately, copolymerization is an effective way to decrease the average sequence length of one certain segments by the incorporation of another component into the copolymer chains.[16] When 1,4-cyclohexanedimethanol (CHDM) is taken as comonomer into the PBT copolymer, the soft segments can be regulated within the acceptable length, and the cyclohexane ring in the synthesized copolymer would surely enhance the thermal stability, mechanical performance, and transparency.[15] The new-type thermoplastic polyester elastomers (TPEEs) would be attractive for the combination of the aromatic polyester advantages, such as excellent mechanical properties and thermal stabilities, and the aliphatic ones, for instance, biodegradability and solubility.[17–20]

However, there has seldom been reported work concerned with electrospinning of PBT and its copolymer, except by Catalani et al.[21] Their research reported that a substantial amount of residual charge in the PBT electrospun fibers was trapped within or at the interface of the crystalline phase. In our study, we first synthesized PBT copolymer with aim of excellent strength and flexibility in the presence of PTMG and CHDM. Then, PBT copolymer fibrous membranes were produced by means of electrospinning. The properties of the resulting product may meet the potential for application of fiber membranes in tissue engineering (e.g., blood vessels)[22] and for filtration under harsh conditions, such as polluted water with bacteria and large flow fluctuation.

Poly[(butylene terephthalate)-*co*-(1,4-cyclohexanedimethanol terephthalate)]-*b*-poly(tetramethylene glycol) (P(BT-*co*-CT)-*b*-PTMG) (PTMG number-average molecular weight = 1000) was synthesized in this article on the basis of PBT and CHDM as rigid segments and PTMG as a flexible segment. The resulted copolymers were divided into two different series: (1) PBT6–Cxpct, where the mass ratio of dimethyl terephthalate (DMT) to PTMG was 6 : 4, and (2) PBT9–Cxpct, where the mass ratio of DMT to PTMG was 9 : 1 and the Cxpct stood for the molar ratio of CHDM to 1,4-butanediol (BDO) at the beginning of the polymerization experiments. For example, the abbreviation PBT6–C10 for the P(BT-*co*-CT)-*b*-PTMG copolymers, that is, PBT6–C10–PTMG4, means that the mass ratio of DMT to PTMG was 6 : 4 and the molar ratio of CHDM to BDO was 10 : 90.

Scanning electron microscopy (SEM), uniaxial tensile testing, differential scanning calorimetry (DSC), and X-ray diffraction (XRD) were used to investigate the morphology, tensile strength, thermal properties, and crystal characteristics of the electrospun fiber membranes, respectively. When the proportion of the soft and rigid segments in the polymeric chains were regulated, the resulting copolymers exhibited different performances, and correspondingly, the electrospun membranes could have had distinct properties.

EXPERIMENTAL

Materials

Commercially available CHDM (Liaohua Petrochemical Co., Liaoyang, China), DMT (Liaohua Petrochemical), BDO (analytical grade, Beijing Chemical Plant, China), PTMG (Yantai Wanhua Group, Yantai, China), and tetrabutyl titanate (analytical grade, Beijing Chemical Plant) were used as received. Irganox 1010, as a stabilizer, was generously provided by the Research Institute of LiaoYang Petrochemical Corporation (Liaoyang, China) Trifluoroacetic acid (TFA; purity $\geq$ 99.0%) and dichloromethane (DCM; purity $\geq$ 99.5%) were purchased from Rizhao Lide Chemical Co. (China) and Beijing Research Institute of Chemical Industry (Beijing, China), respectively. Commercial TPEE (Hytrel 4056) was from Dupont Company (USA). The solvent system used in our work was a mixed solvent of TFA and DCM (8 : 2 v/v). All other chemicals were used without further treatment.

Synthesis of the P(BT-*co*-CT)-*b*-PTMG copolymers

The P(BT-*co*-CT)-*b*-PTMG copolymers (including PBT6–C10, PBT6–C20, PBT9–C20, and PBT9–C25) were synthesized in our laboratory. The transesterification and polycondensation were carried out in a 3-L jacketed stainless steel reactor equipped with a transesterification distillation system to remove the released methanol. The route of transesterification and polycondensation of the P(BT-*co*-CT)-*b*-PTMG copolymers is shown in Figure 1.

As a typical preparation of PBT6–C20, DMT (776 g), BDO (500 g, 5.55 mol), CHDM (200 g, 1.39 mol), PTMG (520 g), Irganox1010 (5.25 g), and tetrabutyl titanate (0.46 g) were charged into a reactor with gentle agitation; the mass ratio of DMT (776 g) to PTMG (520 g) was 6 : 4, and the molar ratio of CHDM (1.39 mol) to BDO (5.55 mol) was 20 : 80. Then, the temperature slowly went up to 215°C for 1 h and stayed at 215°C for another 1 h to reach the end point of the transesterificaton. The temperature of the melt polycondensation was set at 255 $\pm$ 5°C, and the pressure of the reaction system was

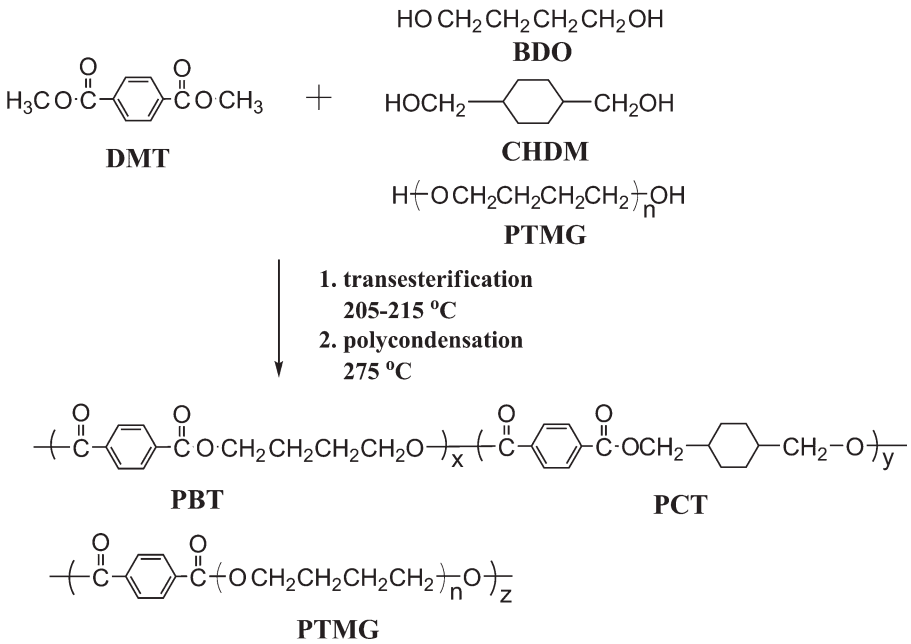

Figure 1 Synthesis route of the P(BT-*co*-CT)-*b*-PTMG copolymers.

gradually reduced, first to 180–200 mmHg over 40 min. For another 20 min, the pressure was further reduced to 60 Pa, and the temperature was increased to the final temperature of 275 ± 5°C and stayed constant for about 2 h with simultaneous removal of ethylene glycol and other volatiles by distillation to acquire copolymers with a satisfactory molecular weight. Finally, the resulting copolymers were taken out of the 3-L jacketed stainless steel reactor under a dry nitrogen atmosphere, cooled to room temperature, dissolved in chloroform, and precipitated by the pouring of the solution into the excess petroleum ether, washing with ethanol, and then drying in a vacuum dryer at 50°C for 24 h to constant mass.

Electrospinning of fiber membranes

The electrospinning apparatus consisted of a plastic syringe, a copper electrode (inner diameter = 0.8 mm), a ground stainless steel plate, and a high-voltage power supply (DW-P303-2AC, Dongwen high voltage power supply co., Tianjin, China) with a low current output (see Fig. 2). All samples, including the synthetic copolymers and commercial TPEE (Hytrel 4056), were dissolved in a mixed solvent of TFA and DCM at room temperature with gentle stirring for 6 h to form a homogeneous solution. First, to observe the concentration effect, the PBT6–C20 fiber membranes were prepared at a fixed voltage of 20 kV and a distance between the spinneret and plate (DBSP) of 15.6 cm, with the solution concentration changed from 24 to 32% w/v. Then, a series of fiber membranes were produced to find the voltage impact on electrospinning at a fixed concentration of 28% w/v and the DBSP still at 15.6 cm. Finally, the copolymers (PBT6–C10, PBT6–C20, PBT9–C20, and PBT9–C25) and Hytrel 4056 fiber membranes were electrospun at a fixed concentration of 28% w/v and a constant applied voltage of 20 kV to observe their mechanical properties.

Characterization

Copolymers

The FTIR spectra were recorded on Nicolet 8700 spectrometer. The copolymer had characteristic adsorptions at 2941 cm^{-1} (—CH_2— asymmetric stretching), 1715 cm^{-1} [—C(O)— stretching], 1620 and 1000 cm^{-1} (characteristic band of phenyl ring), 1470 cm^{-1} (—CH_2— bending), 1269 cm^{-1} [skeletal vibration of ester bond —C(O)—O—], 1103 cm^{-1} (skeletal vibration of ether bond —C—O—C—), and 728 cm^{-1} (—CH_2— rocking). The ^{1}H-NMR spectra were recorded at room temperature on a Bruker AC-600 spectrometer operating at 600 MHz, with tetramethylsilane as an internal standard.

^{1}H-NMR ($CDCl_3$, δ): 1.0–2.2 (proton resonances of the cyclohexylene group in the trans or cis configuration, H^{3e}, H^{3f}, H^{3g}, H^{3h}, and H^{3i}), 1.95 (H^1), 3.39 (H^5, methylene proton resonance in the soft segment), 1.60 (H^6), 4.17 (H^{4t}), 4.28 (H^{4c}), 4.41 (H^2), 4.35 (H^8), 8.07 (H^7, proton resonances of phenyl).

Tensile testing determination of the copolymers was performed with a tensile strain rate of 500 mm/min at room temperature on dog-bone-shaped specimens according to Chinese national standards (GB/T 1040-92). The intrinsic viscosity was

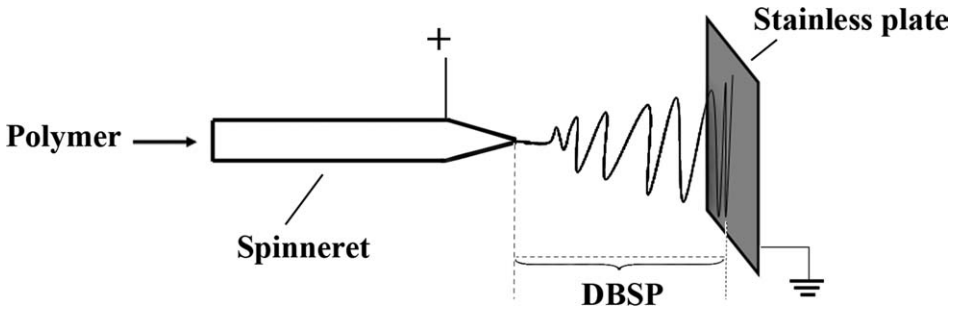

Figure 2 Scheme of the electrospinning apparatus.

measured at 30°C on an Ubbelohde viscometer with a polymer solution of 0.1 g/dL in phenol/tetrachloroethane (60/40 w/w) and calculated according to the one-point method. For the thermal transition process, we used a (PerkinElmer Inc, USA) under nitrogen purge by the following procedure. The samples of PBT9–Cxpct and PBT6–Cxpct were heated at a rate of 40°C/min to the desired JEOL Ltd. temperature to ensure complete melting and kept at this temperature for 3 min. They were then cooled to −100°C with 100°C/min cooling rates before they were reheated to 230 and 200°C at the rate of 20°C/min, respectively.

Electrospun fiber membranes

Morphology. The morphology of the electrospun fiber membranes was analyzed by a field emission SEM instrument (JSM-6360SEM, JEOL Ltd., Japan). All samples were sputter-coated with gold. The average diameter and the diameter distribution were obtained with a custom code image analysis program JEOL SMile View software (version 2.05) to analyze the SEM images.

The porosity (ε)[23] was calculated from the measured average density (ρ) of the samples and the standard density of copolymers (ρ_0):

$$\varepsilon = \left(1 - \frac{\rho}{\rho_0}\right) \times 100$$

Mechanical behavior. A CMT-8102 electromechanical universal testing machine (SANS Co., China) was used for uniaxial tensile testing of the electrospun membranes, and the samples were 5-mm wide and 80-mm long. The samples were directly mounted on the sample clamps and stretched at a strain rate of 20 mm/min. The thickness of the sample was measured by Microscopy (Olympus BX51). For example, we tested one sample at three different places (typically in the middle and two ends) and then got the average value as the final one.

Crystallization and thermal properties. DSC measurements were carried out with a PerkinElmer DSC instrument. Samples (ca. 5 mg) were hermetically sealed in an aluminum pan and heated from room temperature to 350°C at a rate of 10°C/min for thermal observation. XRD measurements, with an X-ray diffractometer with a Cu target and Kα radiation at a scanning rate of 2°/min, enabled differences in the crystal structures of the fiber membranes to be studied.

RESULTS AND DISCUSSION

Polymerization and properties of the copolymers

PBT is usually synthesized via BDO and DMT in industrial processes.[19,20] When the diol BDO was partly substituted by CHDM to modify the thermal and crystal properties, the poly(1,4-cyclohexanedimethanol terephthalate) (PCT) segment of the copolymers was obtained.[24,25] Furthermore, the soft segment of PTMG was added to the copolymers to enhance the flexibility of the product.[13,26]

A series of observations were carried out to determine the properties of the resulted copolymers. The detailed information for the properties of the copolymers is partly shown in Table I. Figure 3 shows a typical ^{1}H-NMR spectrum of as-synthesized PBT6–C20. The composition of the copolymers could be quantified according to the ^{1}H-NMR spectrum.[15,27] The peaks marked as 2 and 5 with the chemical shifts 4.41 and 3.39 were ascribed to the methylene proton resonances of the hard-segment PBT and soft-segment PTMG. The splits with the chemical shifts 4.18 and 4.28 were assigned as the peaks of methylene protons in CHDM with trans and cis conformations with the subscripts 4t and 4c independently. The molar ratio of PBT, PCT, and PTMG in PBT6–C20 could be obtained through the relative integral intensity of the peaks (I) in the ^{1}H-NMR spectrum. Thus, the mass content of the rigid segment in PBT6–C20 (W) was calculated by the following equation:

$$\begin{aligned} W &= \frac{\text{PBT} + \text{PCT}}{\text{PBT} + \text{PCT} + \text{PTMG}} \times 100\% \\ &= \frac{220I_2 + 274(I_{4c} + I_{4t})}{220I_2 + 274(I_{4c} + I_{4t}) + 1164I_8} \times 100\% \\ &= 57.4\% \end{aligned}$$

TABLE I
Basic Parameters of P(BT-*co*-CT)-*b*-PTMG Copolymers: Melting Temperature (T_m), Intrinsic Viscosity ([η]), *W* Values, Tensile Strength, and Elongation at Break

	T_m (°C)	[η] (dL/g)	*W* (%)	Tensile strength (MPa)	Elongation at break (%)
PBT6–C10	173	1.04	56.9	18.0	1280
PBT6–C20	162	0.74	57.4	20.8	1210
PBT9–C20	183	0.76	91.7	25.3	580
PBT9–C25	181	0.78	91.1	24.6	530

where 220, 274, and 1164 stand for the number-average molecular weights of the repeat units of PBT, PCT, and PTMG, respectively, in PBT6–C20.

The theoretical yield of PBT6–C20 could be calculated on the basis of the relative integral intensity of the peaks in ^{1}H-NMR whose ratio symbolized the molar ratio. The ratio of weight was obtained by multiplication of the ratio of PBT, PCT, and PTMG [I_2:(I_{4c} + I_{4t}):I_8] with the corresponding molar weight, and thus, we got the theoretical yield of 70.6%. However, the wall-adhering phenomenon existed in the melt polycondensation. In fact, we only obtained 63.0% product because about 5–10% of the product adhered on the inner surface of the reactor.

Morphology of the electrospun membranes

The variables, including solution properties, applied electric field, solution flow feeding rate, and DBSP, and other factors, such as the curing temperature, played important roles in the morphology and the performances of the electrospun membranes.[4,5,7,28] Figure 4 shows the typical SEM images of the electrospun fiber membranes. The SEM photographs clearly show that no beads occurred on the fibers electrospun from the PBT6–C20 copolymers, although the applied voltages changed from 16 to 24 kV; this led us to conclude that the PBT6–C20 copolymers had a good spinnability for the range of voltages mentioned previously. Also, for other synthetic copolymers, including PBT6–C10, PBT9–C20, and PBT9–C25, similar results were found, that beads occurred on the SEM images when the voltages changed from 16 to 24 kV. When the applied voltages increased from 16 to 24 kV at a fixed PBT6–C20/(TFA and DCM) solution concentration of 28% w/v, the average diameters of the fibers showed a decreasing trend. The corresponding diameters of the fibers were 1.196, 1.017, 1.091, 0.953, and 0.899 μm. In this case, as the voltage increased, the electrospun solution obtained more charges, and the

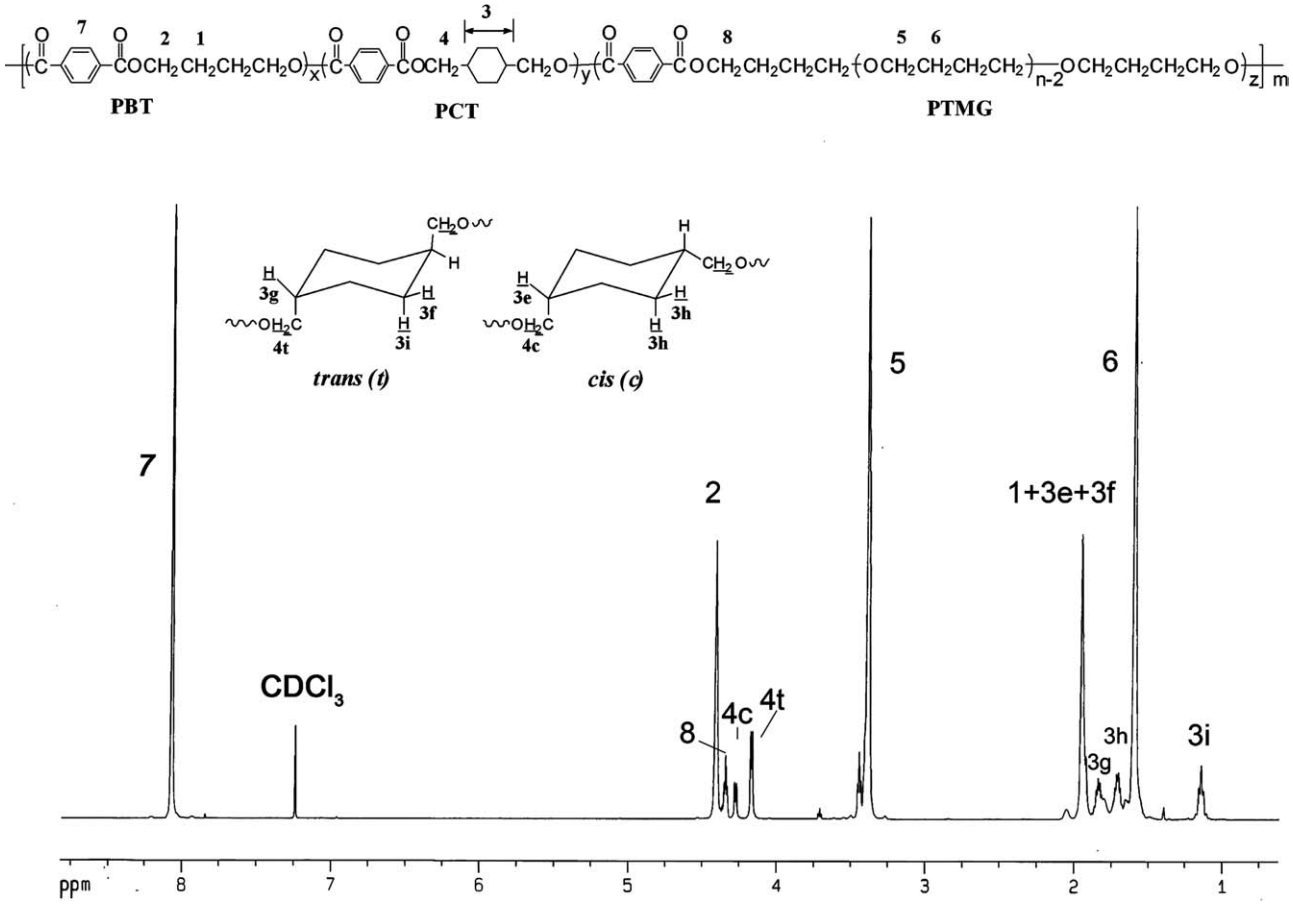

Figure 3 ^{1}H-NMR spectrum of PBT6–C20.

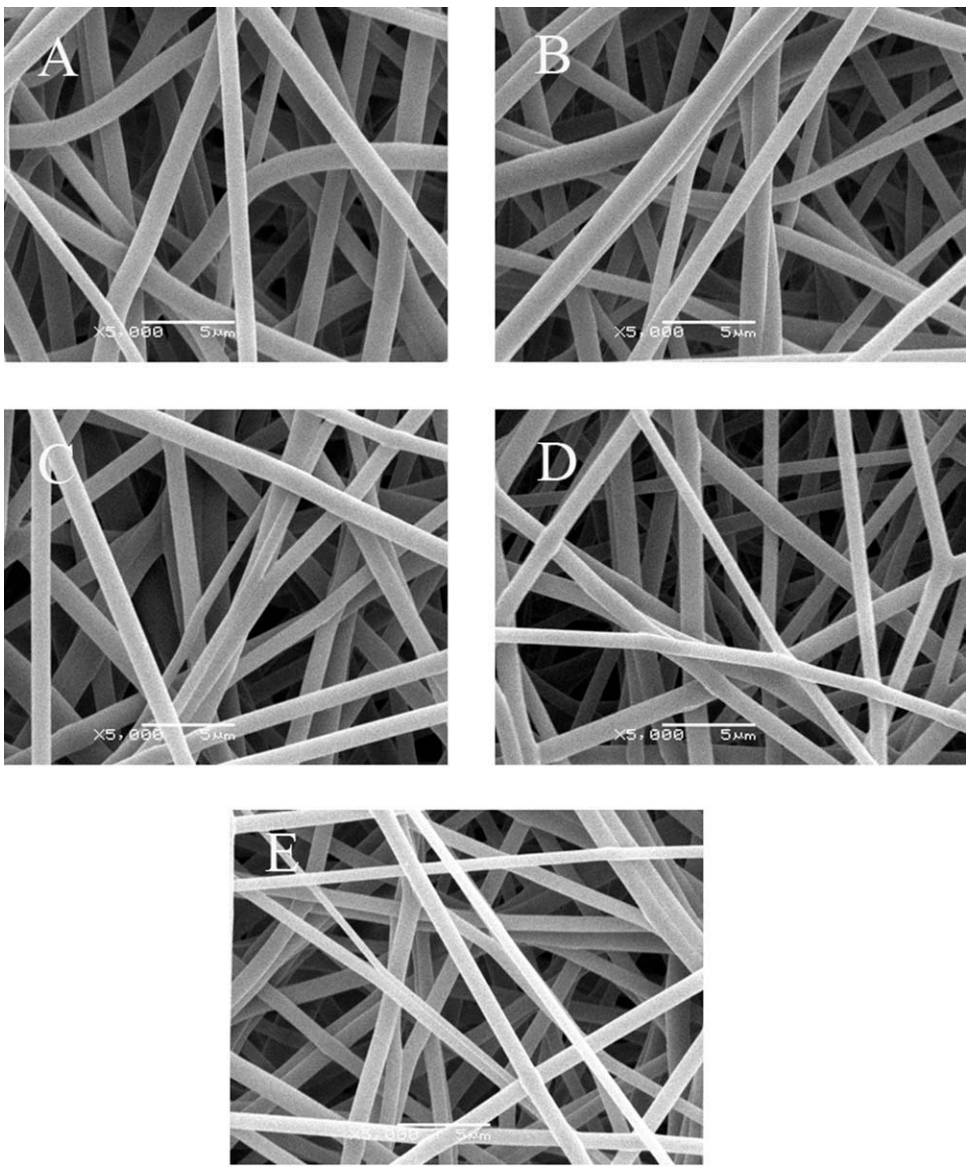

Figure 4 SEM images of the electrospun PBT6–C20 nanofiber membrane. Applied voltage: (A) 16, (B) 18, (C) 20, (D) 22, and (E) 24 kV.

repulsion effect of the jet became stronger; hence, the capability of splitting into thinner fibers was enhanced.

Researchers[29] observed a similar finding: when the initial copolymer concentration increased, a higher diameter was obtained. However, the effect of the concentration on the fiber diameters of the electrospun membranes was quite different with the voltage effect. When we looked at the PBT6–C20/(TFA and DCM) solution, the diameter increased by 34% from a 24 to a 32% w/v solution concentration (see Table II). With increasing copolymer concentration, it was difficult for the fluid to be split into fibers with small diameters because of the increase of the viscosity and the surface tension. This resulted in the larger average diameter. Moreover, for all electrospun copolymers (including PBT6–C10, PBT6–C20, PBT9–C20, and PBT9–C25), the resulting fibers showed diameters of generally less than 1 μm as long as the concentration of electrospun solution was not higher than 30% w/v.

The high porosity with regard to applications, especially for tissue engineering as the extracellular matrix (ECM), protected clothing, and nanofiltration,[30–32] is considered as an indispensable

TABLE II
Fiber Diameters of the Electrospun PBT6–C20/(TFA and DCM) Solutions with Different Concentrations (w/v) at a Fixed Voltage of 20 kV

Concentration (%; w/v)	24	26	28	30	32
Thickness (mm)	0.72	0.50	0.48	0.34	0.66
Average diameter (μm)	0.789	0.783	0.848	0.955	1.055

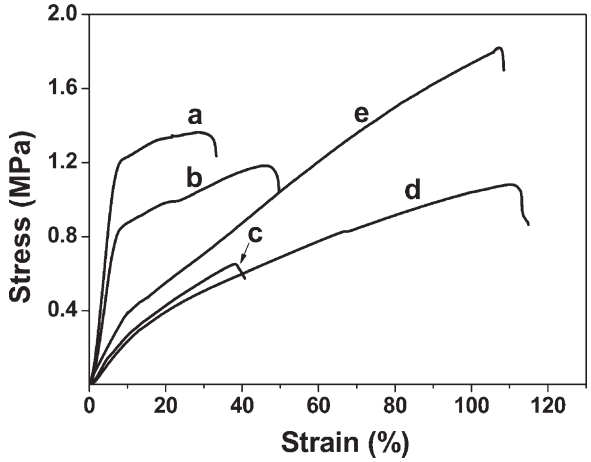

Figure 5 Tensile stress–stain curves of the electrospun P(BT-*co*-CT)-*b*-PTMG copolymers and commercial TPEE fiber membranes with a concentration of 28% w/v and a voltage of 20 kV: (a) PBT9–C25, (b) PBT9–C20, (c) PBT6–C20, (d) PBT6–C10, and (e) commercial TPEE (Hytrel 4056).

characteristic of fiber membranes. The porosity of the electrospun membranes in this study was observed at a fixed solutions concentration of 28% w/v and at a constant voltage of 20 kV. The overall porosity reached 78 ± 6%; the porosity of fiber membranes prepared by PBT6–C10, PBT6–C20, PBT9–C20, and PBT9–C25 was 85, 72, 77, and 75%, respectively. The thickness of the fiber membranes above ranged from 0.32 to 0.67 mm, and the average value was 0.54 mm.

Mechanical properties of the fiber membranes

The mechanical properties of the synthetic copolymer membranes (PBT6–C10, PBT6–C20, PBT9–C20, and PBT9–C25) and commercial TPEE (Hytrel 4056) membranes were compared at a fixed concentration of 28% w/v and at an applied voltage of 20 kV. As shown in Figure 5, the stress–stain curves were divided into three groups by elastic modulus: electrospun PBT9–Cxpct copolymer membranes went first, followed by commercial TPEE (Hytrel 4056) and the PBT6–Cxpct copolymers. The electrospun PBT9–Cxpct copolymer membranes, including PBT9–C20 and PBT9–C25, showed an average elastic modulus higher than the 4.51 ± 0.35 MPa of commercial TPEE (Hytrel 4056).

The fiber membranes of the PBT9–Cxpct copolymers had a larger tensile strength and elastic modulus than those of the PBT6–Cxpct copolymers because of the higher content of PBT segments in the polymeric chains. Moreover, for a certain series of copolymers (e.g., PBT9–Cxpct), the electrospun PBT9–C20 membranes had a tensile strength of 1.18 ± 0.26 MPa and an elastic modulus of 16.73 ± 1.48 MPa, with an increase in the tensile strength to 1.35 ± 0.18 MPa and elastic modulus to 19.48 ± 2.02 MPa for PBT9–C25 membranes. This result demonstrated that the increase of the PCT rigid segment in copolymer chains improved the mechanical performance of copolymer membranes when the content of the PBT segments in P(BT-*co*-CT)-*b*-PTMG copolymers remained relatively constant. However, the tensile strength of PBT6–C10 decreased from 1.08 ± 0.11 to 0.65 ± 0.13 MPa for PBT6–C20 as the content of PCT increased. The reason for this specific phenomenon was presumably that the cyclohexane ring had a negative effect on the motion of polymeric chains as the content of CHDM (PCT) reached a specific proportion of PBT and PTMG.

However, the data from tensile testing showed the behavior of the electrospun copolymers to be distinctly different from that of the bulk copolymers (see tensile information in Tables I and III). When the electrospun membranes were applied to tensile testing, the displacement (or slip) occurred on fibers. This was probably one reason why the bulk material had better tensile results than that of electrospun ones. For the other factor, the electrospun copolymers only had a density of about 20% that of the bulk.

Moreover, the electrospun membranes of the synthetic copolymers had a lower elongation at break (maximum ≈ 120%) than that of the as-synthesized copolymers (minimum = 530%). This result suggested that the electrospun membranes broke before they could exhibit the tensile properties of the bulk because of the displacement and fracture of fibers. This seemingly premature failure was similar to the work of Pedicini and Farris.[33]

Thermal properties and crystal structure of the electrospun membranes

Yokouchi et al.[34] demonstrated that PBT has two crystal modifications, the α and β forms; the latter form exists only under tension and consists of more

TABLE III
Tensile Properties of the Fiber Membranes Electrospun from Five Samples [PBT6–C10, PBT6–C20, PBT9–C20, PBT9–C25, and Commercial TPEE (Hytrel 4056)]

	PBT6–C10	PBT6–C20	PBT9–C20	PBT9–C25	Hytrel 4056
Elastic modulus (MPa)	2.81 ± 0.17	3.12 ± 0.41	16.73 ± 1.48	19.48 ± 2.02	4.51 ± 0.35
Tensile strength (MPa)	1.08 ± 0.11	0.65 ± 0.13	1.18 ± 0.26	1.35 ± 0.18	1.82 ± 0.14

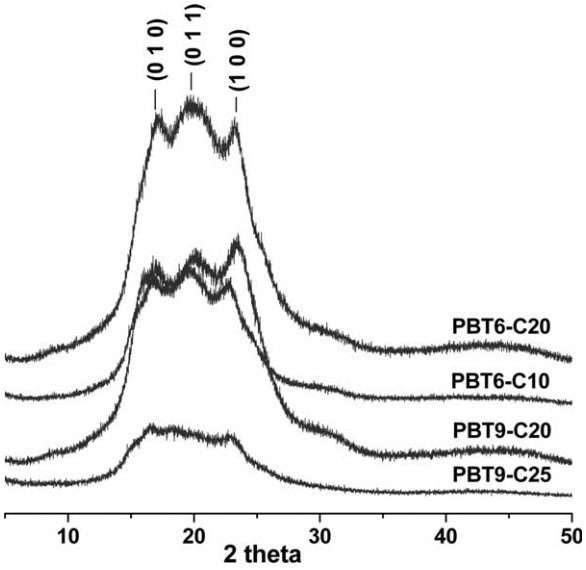

Figure 6 WAXD pattern of the electrospun P(BT-*co*-CT)-*b*-PTMG copolymer nanofiber membranes.

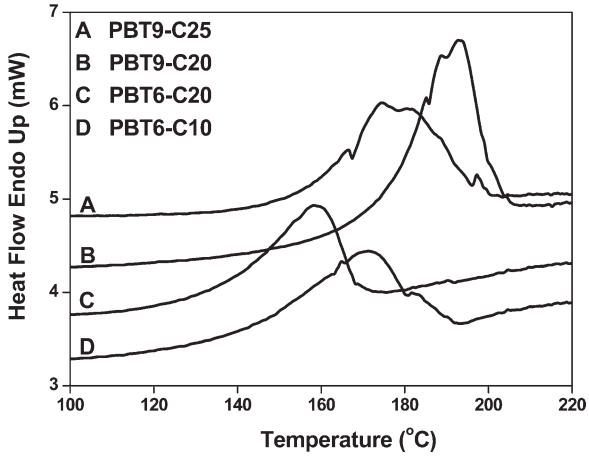

Figure 7 DSC thermograms of the electrospun P(BT-*co*-CT)-*b*-PTMG copolymer nanofiber membranes: (A) PBT9–C25, (B) PBT9–C25, (C) PBT6–C20, and (D) PBT6–C10.

extended molecular chains. The transition between the α form and β form takes place reversibly by stretching and relaxation.

The study was carried out over an angle range of 3–50°. The wide-angle XRD patterns of the P(BT-*co*-CT)-*b*-PTMG copolymer fiber membranes are shown in Figure 6. The three large peaks on the figure were evidence of the fact that the samples contained a crystalline phase in the P(BT-*co*-CT)-*b*-PTMG copolymer fiber membranes, including PBT6–C10, PBT6–C20, PBT9–C20, and PBT9–C25. For the PBT9–C20 copolymer fiber membranes, the plot showed three strong diffraction peaks at 17.02, 20.00, and 23.36°. These peaks corresponded to the (0, 1, 0), (0, 1, 1), and (1, 0, 0) diffraction planes of the α form of PBT with a triclinic configuration.[35] Furthermore, Figure 6 indicates that structural change occurred in PBT with the incorporation of PCT and PTMG. The interplanar spacing (*d*) values for various peaks of PBT were obtained from Bragg's law and Scherrer's equation:[36]

$$d = \lambda/2 \sin \theta$$

Where θ stands for the half value of Bragg angles (2θ) with the increase of PCT content and the decrease of PBT content in the copolymer chain, the PBT α form was gradually destroyed. For example, the *d* values for the fibers of PBT9–C20 and PBT9–C25 (5.51 Å, 5.35 Å) were close to the characteristic peaks (5.60 Å) at the (0, −1, 1) diffraction plane compared with those of PBT6–C10 and PBT6–C20 (5.30 and 5.18 Å, respectively). More detailed information about the peak parameters of the plot is shown in Table IV.

The DSC thermograms of the electrospun P(BT-*co*-CT)-*b*-PTMG copolymer fiber membranes are shown in Figure 7. The electrospun membranes of the PBT9–Cxpct copolymer maintained a higher melting point than that of PBT6–Cxpct copolymer membranes; this was attributed to the higher content of PBT rigid segments in the copolymer chains. On the DSC curves, the endothermic peaks of electrospun PBT9–C25 and PBT9–C20 were at 175 and 193°C, respectively, whereas the peaks of PBT6–C20 and PBT6–C10, at 158 and 171°C, respectively, were lower than those of the electrospun PBT9–Cxpct membranes mentioned previously.

The enthalpy of meting of the electrospun PBT6–C10 membrane was 24.5 J/g, whereas that of the electrospun PBT6–C20 membrane was 21.5 J/g. This lower fusion heat of the PBT6–C20 membrane was probably due to the higher content PCT segments,

TABLE IV
Peak Parameters of P(BT-*co*-CT)-*b*-PTMG Copolymer Membranes from Figure 5

	PBT6–C10/PBT6–C20/PBT9–C20/PBT9–C25											
Peak number	Angle of X-ray scattering 2θ (°)				*d* (Å)				Relative intensity (%)			
1	17.10	17.09	16.08	16.55	5.30	5.18	5.51	5.35	70.7	84.9	45.6	100
2	19.38	19.30	17.02	18.28	4.58	4.60	5.20	4.85	68.8	7.8	39.1	20.9
3	22.78	20.55	20.00	19.95	3.90	4.32	4.44	4.45	100	0.2	48.1	0.6
4	–	23.29	23.36	22.81	–	3.82	3.81	3.90	–	100	100	97.4
5	30.74	31.26	30.81	41.60	2.91	2.86	2.80	2.17	0	1.8	1.6	2.6

which had a negative effect on the formation of the crystal in the copolymers as the content of CHDM increased in the copolymers. The results of the electrospun PBT9–Cxpct (PBT9–C20 and PBT9–C25) membranes involving the fusion heat were similar to that of PBT6–Cxpct (PBT6–C10 and PBT6–C20).

In general, the DSC diagrams agreed with the XRD results that the crystalline phase existed in the electrospun P(BT-*co*-CT)-*b*-PTMG copolymer fiber membranes. A higher content of PBT rigid segments in the copolymer chains enabled the electrospun copolymer membranes to have a higher melting point. However, for a certain series of copolymers, for example, PBT6–Cxpct, the fusion heat of the electrospun membranes decreased as the content of PCT segments increased in the copolymers.

CONCLUSIONS

The P(BT-*co*-CT)-*b*-PTMG copolymers (PBT6–C10, PBT6–C20, PBT9–C20, and PBT9–C25) were synthesized and subsequently electrospun to fiber membranes in our research. As the concentration increased, the diameter of the fibers kept an increasing trend. However, the applied voltages took an opposite trend compared with the concentration. The XRD and DSC diagrams showed that the crystalline phase existed in the electrospun P(BT-*co*-CT)-*b*-PTMG copolymer fiber membranes. A higher content of PBT rigid segments in the copolymer chains enabled the electrospun copolymer membranes to have a higher melting point. For a certain series of copolymers, for example, PBT6–Cxpct, the fusion heat of electrospun membranes decreased as the content of PCT segments increased in the copolymers. Compared with commercial TPEE (Hytrel 4056), the electrospun membranes of the PBT9–Cxpct copolymers, including PBT9–C20 and PBT9–C25, had a higher elastic modulus. However, the electrospun membranes of commercial TPEE had a higher tensile strength than that of the synthetic copolymers in this study. Furthermore, the fiber membranes of the PBT9–Cxpct copolymers had a higher tensile strength and elastic modulus than those of the PBT6–Cxpct copolymers as the content of the PBT segment in copolymers increased. In summary, the electrospun P(BT-*co*-CT)-*b*-PTMG copolymer fiber membranes would probably have potential for application in filtration in the nanometer scale and for tissue engineering because of their three-dimensional interconnected structure and acceptable performance in thermal and tensile aspects.

References

1. Formhals, A. U.S. Pat. 1,975,504 (1934)
2. Zhang, B.; Li, C.; Chang, M. Polym J 2009, 41, 252.
3. Shin, Y. M.; Hohman, M. M.; Brenner, M. P.; Rutledge, G. C. Polymer 2001, 42, 09955.
4. Fong, H.; Chun, I.; Reneker, D. Polymer 1999, 40, 4585.
5. Lee, K. H.; Kim, H. Y.; Khil, M. S.; Ra, Y. M.; Lee, D. R. Polymer 2003, 44, 1287.
6. Tan, S. H.; Inai, R.; Kotaki, M.; Ramakrishna, S. Polymer 2005, 46, 6128.
7. Demir, M. M.; Yilgor, I.; Yilgor, E.; Erman, B. Polymer 2002, 43, 3303.
8. Reneker, D. H.; Yarin, A. L.; Fong, H.; Koombhongse, S. J Appl Phys 2000, 87, 4531.
9. Hohman, M. M.; Shin, M.; Rutledge, G.; Brenner, M. P. Phys Fluids 2001, 13, 2201.
10. Zong, X.; Kim, K.; Fang, D.; Ran, S.; Hsiao, B. S.; Chu, B. Polymer 2002, 43, 4403.
11. Hou, H.; Jun, Z.; Reuning, A.; Schaper, A.; Wendorff, J. H.; Greiner, A. Macromolecules 2002, 35, 2429.
12. Groitzsch, D.; Fahrbach, E.; U.S. Pat. 4,618,524 (1986).
13. Park, Y. H.; Cho, C. G. J Appl Polym Sci 2001, 79, 2067.
14. Schollenberger, C. S. Polyurethane Technology; Interscience: New York, 1979.
15. Zhang, Y.; Feng, Z.; Feng, Q.; Cui, F. Polym Degrad Stab 2004, 85, 559.
16. Zhang, Y.; Feng, Z.; Zhang, A. Polym Int 2003, 52, 1351.
17. Deng, L.-M.; Wang, Y.-Z.; Yang, K.-K.; Wang, X.-L.; Zhou, Q.; Ding, S.-D. Acta Mater 2004, 52, 5871.
18. Ding, B.; Kim, H. Y.; Lee, S. C.; Shao, C. L.; Lee, D. R.; Park, S. J.; Kwag, G. B.; Choi, K. J. J Polym Sci Part B: Polym Phys 2002, 40, 1261.
19. Jin, H.-J.; Chen, J.; Karageorgiou, V.; Altman, G. H.; Kaplan, D. L. Biomaterials 2004, 25, 1039.
20. Li, M.; Guo, Y.; Wei, Y.; MacDiarmid, A. G.; Lelkes, P. I. Biomaterials 2006, 27, 2705.
21. Catalani, L.; Collins, G.; Jaffe, M. Macromolecules 2007, 40, 1693.
22. Potter, W. G. Epoxide Resins; Springer: New York, 1970.
23. Vaz, C. M.; van Tuijl, S.; Bouten, C. V. C.; Baaijens, F. P. T. Acta Biomater 2005, 1, 575.
24. Lee, H. S.; Park, H. D.; Cho, C. K. J Appl Polym Sci 2000, 77, 699.
25. Zhang, Y.; Feng, Z.; Feng, Q.; Cui, F. Eur Polym J 2004, 40, 1297.
26. Shi, Y.; Wu, M. Polym Int 1995, 38, 357.
27. Kricheldorf, H.; Al Masri, M.; Lomadze, N.; Schwarz, G. Macromolecules 2005, 38, 9085.
28. Reneker, D.; Chun, I. Nanotechnology 1996, 7, 216.
29. Vrieze, S. D.; Westbroek, P.; Camp, T. V.; Clerck, K. D. J Appl Polym Sci 2010, 115, 837.
30. Zhu, X.; Cui, W.; Li, X.; Jin, Y. Biomacromolecules 2008, 9, 1795.
31. Burger, C.; Hsiao, B.; Chu B. Annu. Rev. Mater. Res. 2006, 36, 333.
32. Ndreu, A.; Nikkola, L.; Ylikauppila, H.; Ashammakhi, N.; Hasirci, V. Nanomedicine 2008, 3, 45.
33. Pedicini, A.; Farris, R. J. Polymer 2003, 44, 6857.
34. Yokouchi, M.; Sakakibara, Y.; Chatani, Y.; Tadokoro, H.; Tanaka, T.; Yoda, K. Macromolecules 1976, 9, 266.
35. Li, R. K. Y.; Tjong, S. C.; Xie, X. L. J Polym Sci Part B: Polym Phys 2000, 38, 403.
36. Alexander, L. X-Ray Diffraction Methods in Polymer Science; Wiley: New York, 1969.